Supplementary materials

Improving the stability and performance of perovskite solar cells via off-the-shelf post-device ligand treatment

Hong Zhang[1], Xingang Ren[1], Xiwen Chen[2], Jian Mao[1], Jiaqi Cheng[1], Yong Zhao[1], Yuhang Liu[3], Jovana Milic[3], Wan-Jian Yin[2], Michael Grätzel[3], Wallace C. H. Choy[1,*]

[1] Department of Electrical and Electronic Engineering, The University of Hong Kong, Pok Fu Lam Road, Hong Kong SAR, China

[2] Soochow Institute for Energy and Materials Innovations (SIEMIS), College of Physics, Optoelectronics and Energy & Collaborative Innovation Center of Suzhou Nano Science and Technology, Soochow University, 215006, Suzhou, China

[3] Laboratory for Photonics and Interfaces, Institute of Chemical Sciences and Engineering, School of Basic Sciences, Ecole Polytechnique Fédérale de Lausanne, CH-1015 Lausanne, Switzerland.

E-mail: chchoy@eee.hku.hk

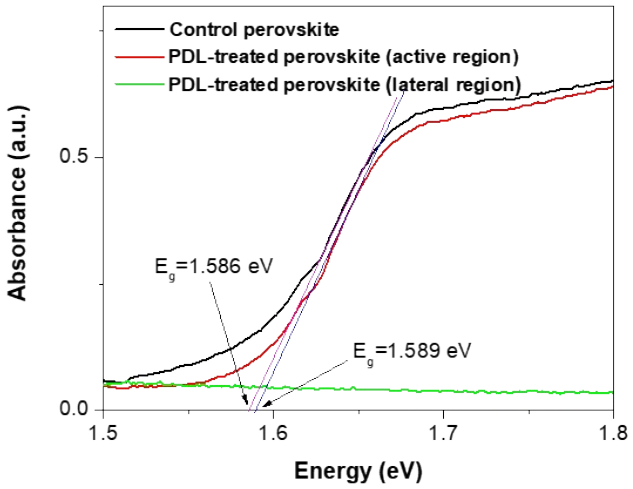

Fig. S1 Zoom-in on the onset of absorption in Fig. 1b.

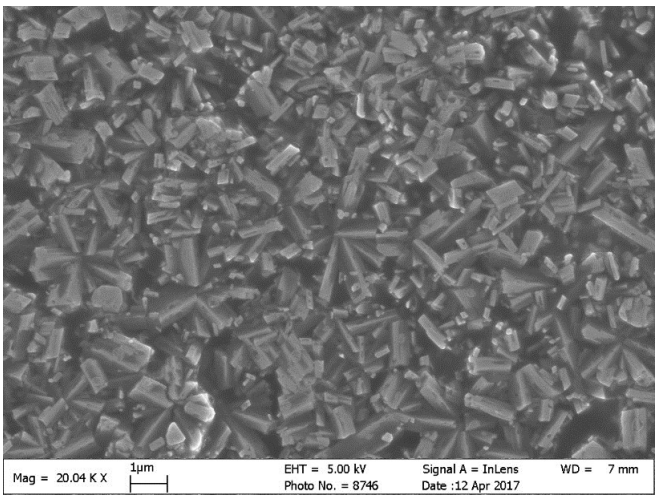

Fig. S2 Top-view SEM image of the perovskite materials in the lateral region after PDL treatment.

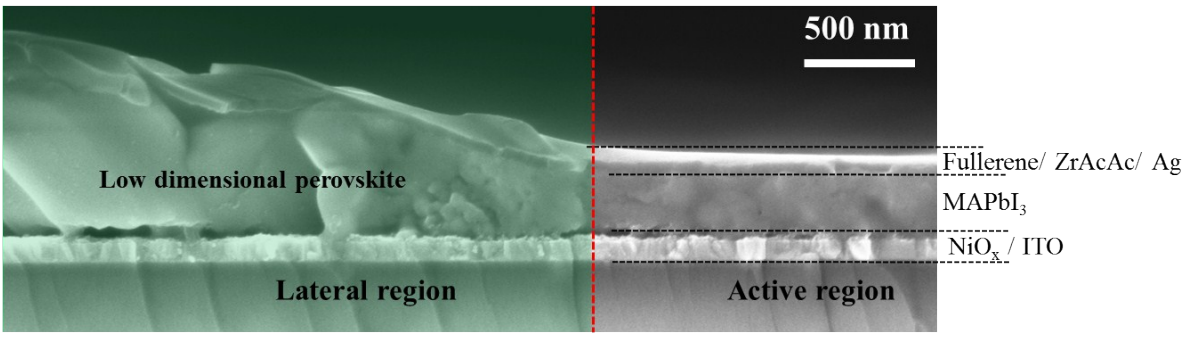

Fig. S3 Cross-sectional SEM image of the PVSCs after PDL treatment.

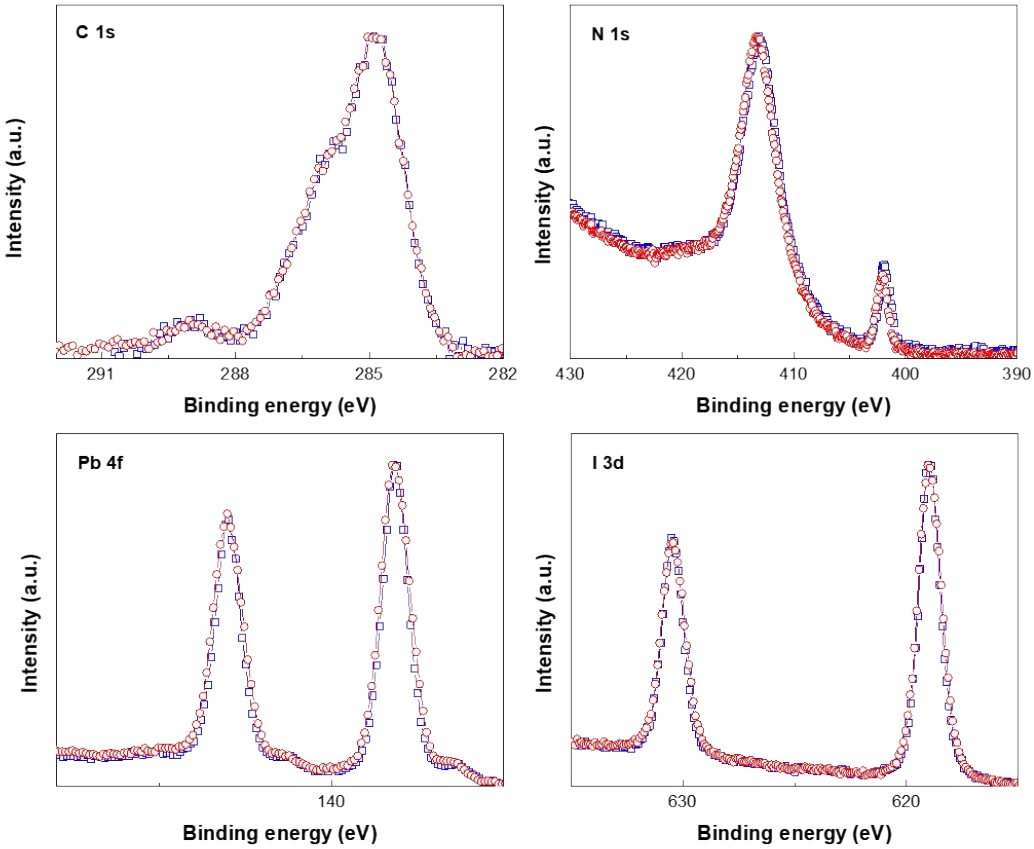

Fig. S4 XPS peak of C 1s, N 1s, Pb 4f, and I 3d spectra obtained from the surface of as-prepared perovskite film (***blue color***) and perovskite removal by tape and chlorobenzene washing (***red color***).

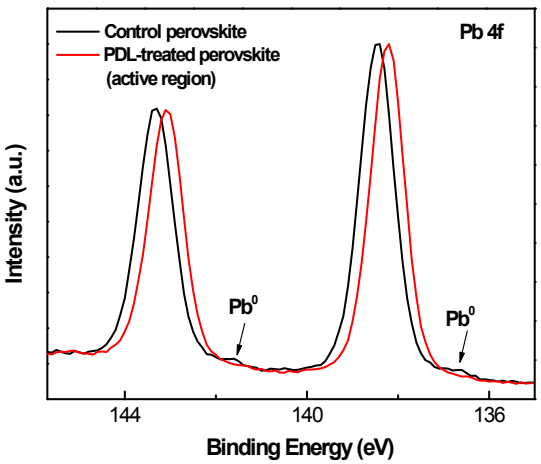

Fig. S5 XPS peak of Pb 4f obtained from the surface of control perovskite film without any treatment and the covered (active-region) perovskite with PDL treatment.

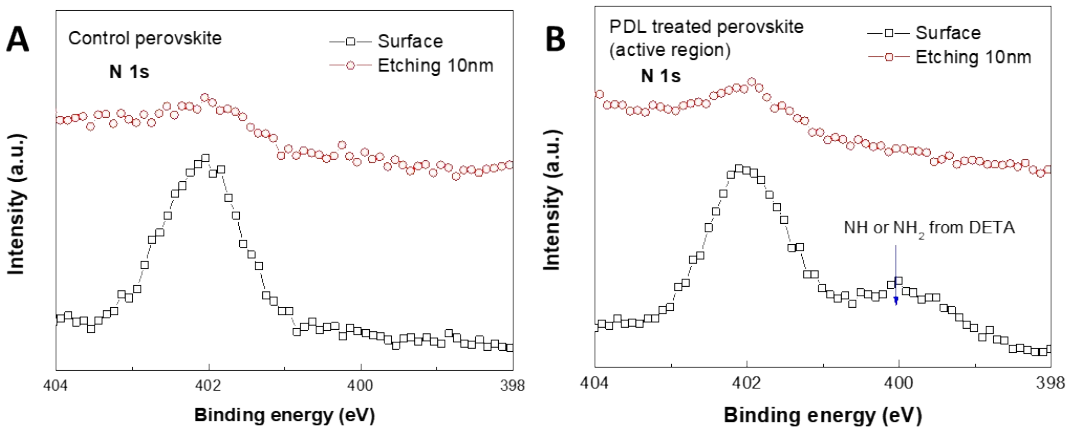

Fig. S6 XPS peak of N 1s obtained from the surface and 10 nm depth of control perovskite film without any treatment and the covered (active-region) perovskite with PDL treatment.

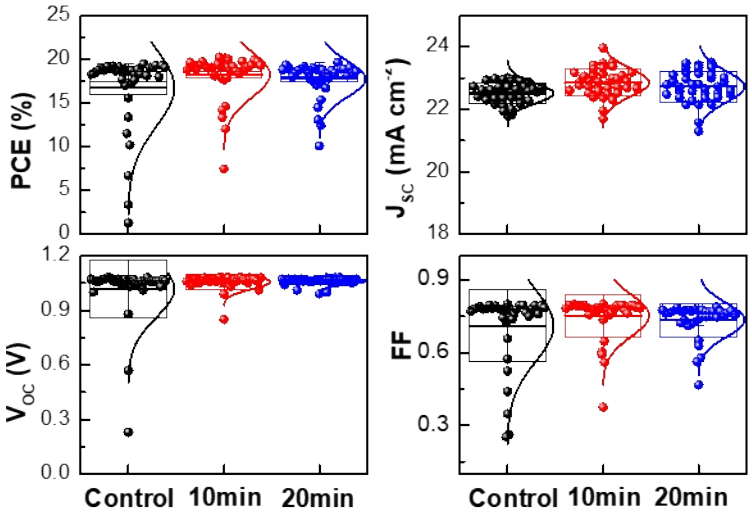

Fig. S7 Photovoltaic metrics of devices plotted as a function of duration of PDL treatment (37 cells were fabricated and tested).

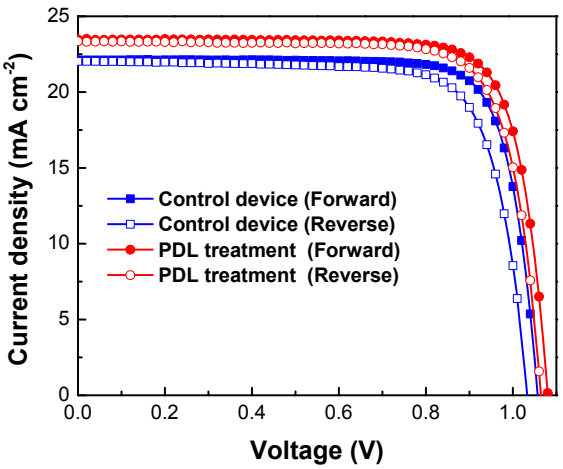

Fig. S8 *J-V* curves of the PVSC (device A) measured under different scan directions.

Table S1. Photovoltaic parameters of PVSCs (device A) measured under different scan directions.

PDL treatment	J_{sc} **(mA cm^{-2})**	V_{oc} **(V)**	**FF (%)**	**PCE (%)**
Before (F)	22.12	1.06	79.6	18.67
Before (S)	22.03	1.03	76.9	17.44
After (F)	23.47	1.08	79.4	20.13
After (S)	23.35	1.06	78.5	19.44

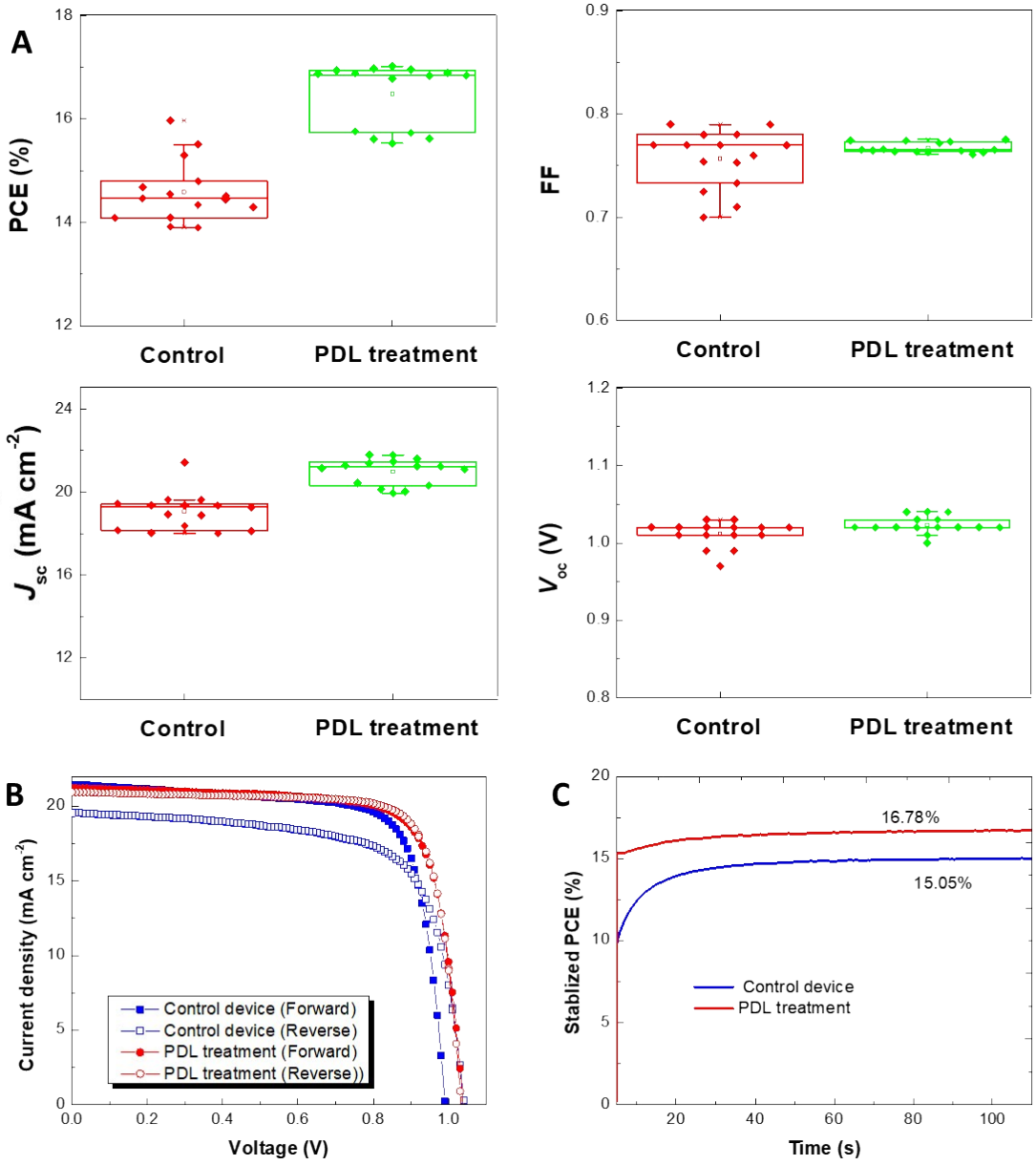

Fig. S9 (a) Photovoltaic metrics of $Cs_5(MA_{0.17}FA_{0.83})_{95}Pb(I_{0.83}Br_{0.17})_3$ PVSCs plotted as a function of duration of PDL treatment. (b) *J-V* curves and (c) the relevant steady-state PCE of a typical $Cs_5(MA_{0.17}FA_{0.83})_{95}Pb(I_{0.83}Br_{0.17})_3$ PVSCs without and with PDL treatment. The scan rate is 0.1V/s. 15 cells were fabricated and tested.

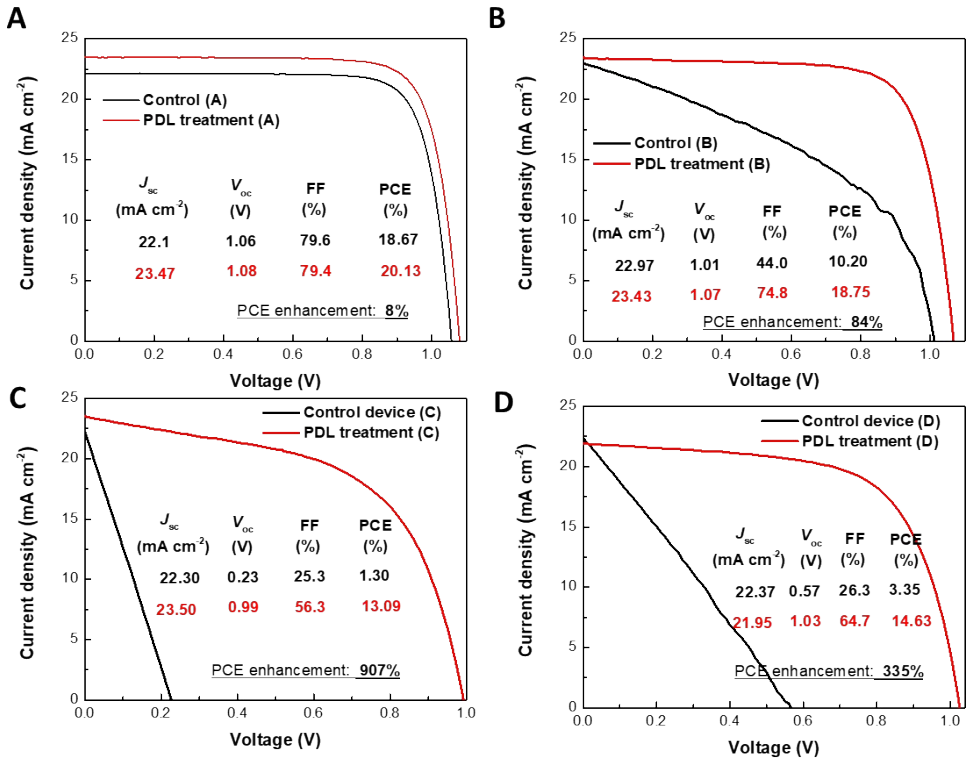

Fig. S10 *J-V* curves of some typical PVSCs (device A to D) in Fig. S6.

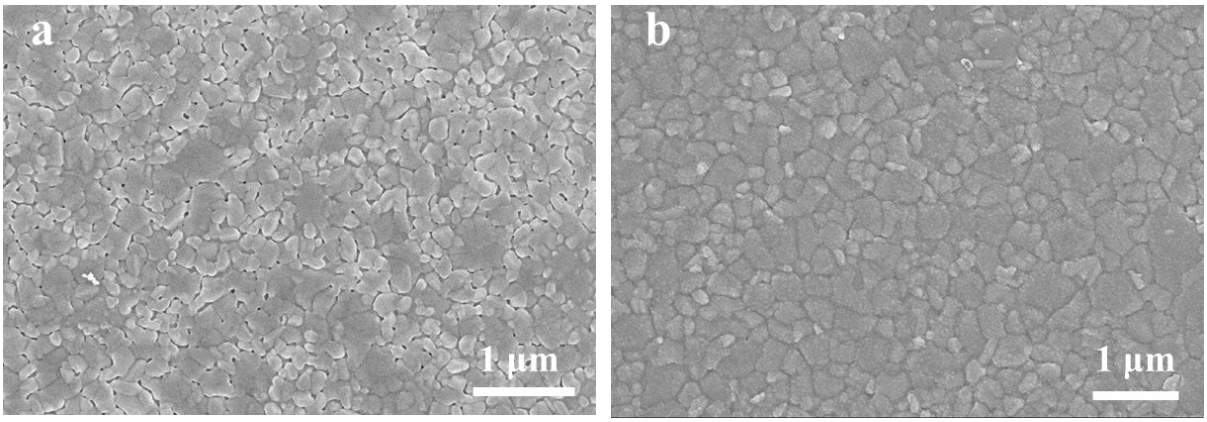

Fig. S11 Top-view SEM images of perovskite film in a 'poor' PVSC (a) without (b) with LPD modification. The produced CH_3NH_2 gas during PDL treatment process can heal the defects (or pin-holes) of active region through the following reaction:

$$CH_3NH_3PbI_3(s) + CH_3NH_2(g) \xrightarrow{25℃} CH_3NH_3PbI_3.xCH_3NH_2(l)(s) \xrightarrow{25℃} CH_3NH_3PbI_3(s) + CH_3NH_2(g)$$

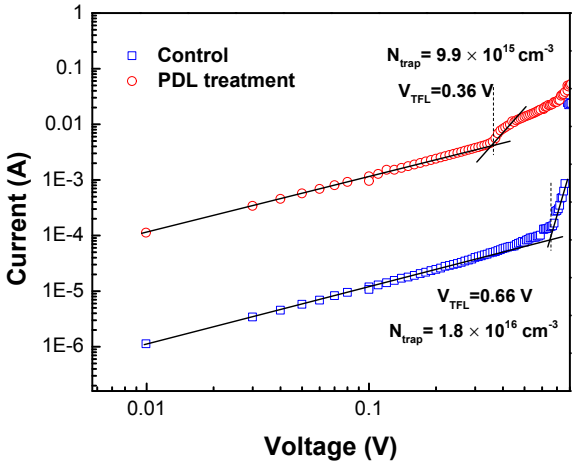

Fig. S12 Trap states density of perovskite films as determined by space-charge-limited current (SCLC) method using the electron-only device with the configuration of ITO/SnO_2/$CH_3NH_3PbI_3$(Cl)/C_{60}/BCP/Ag. The trap density N_{trap} is determined by the equation: $V_{TFL}=eN_{trap}L^2/(2\varepsilon\varepsilon_0)$, where V_{TFL} is the trap-filed limit voltage; L is the thickness of perovskite; ε is the relative dielectric constant of perovskite; ε_0 is the vacuum permittivity.

Notes for DFT calculations

We did not consider the MAI termination since previous reports from both experiments and theories had indications that PbI_2-terminated [001] surface is more stable. For examples, in experiment, Lindblad *et al* [1] reported that a small understoichiometry in I and N atoms for the two-step synthesis of the TiO_2/$MAPbI_3$ interface, which indicates that surface is CH_3NH_3-poor. In theory, Haruyama *et al*[2] pointed out that (001) surface of tetragonal surface are flat nonpolar surface, which consists of alternate stacking of the neutral $[MAI]^0$ and $[PbI_2]^0$ planes. The (100) surface is constructed with stacking of the $[MAPbI]^{2+}$ and $[I_2]^{2-}$ layers, while the $[MAI_3]^{2-}$ and $[Pb]^{2+}$ layers compose the (101) surface. The calculations on surface energy show that nonpolar surface is much more stable than nonpolar surface. In conclusion, we choose PbI_2-teminated (001) surface since it is the most stable and common surface for $MAPbI_3$ from both experiment and theory.

The contributions of density of states of $MAPbI_3$ surface have been extensively studied in Haruyama *et al* 's work. Basically, the surface states are within the band gap, which is benign for carrier recombination. However, the bandgap at surface area will be enlarged. The effect of DETA is to passivate surface by reducing its bandgap (see Fig. S14a,b).

Defect calculations on bulk $MAPbI_3$[3] show that the dominating defects are Pb vacancy and MA interstitial while MA vacancy has much larger formation energy. Considering that PbI_2-terminated surface is intrinsically MA poor, we choose Pb vacancy for the study. We double checked the formation energies of Pb and MA vacancies on PbI_2-terminated (001) surface and found that the Pb vacancy are still dominating defects on surface. As shown in Fig. S14c, DETA passivation can reduce the trap states near band edge.

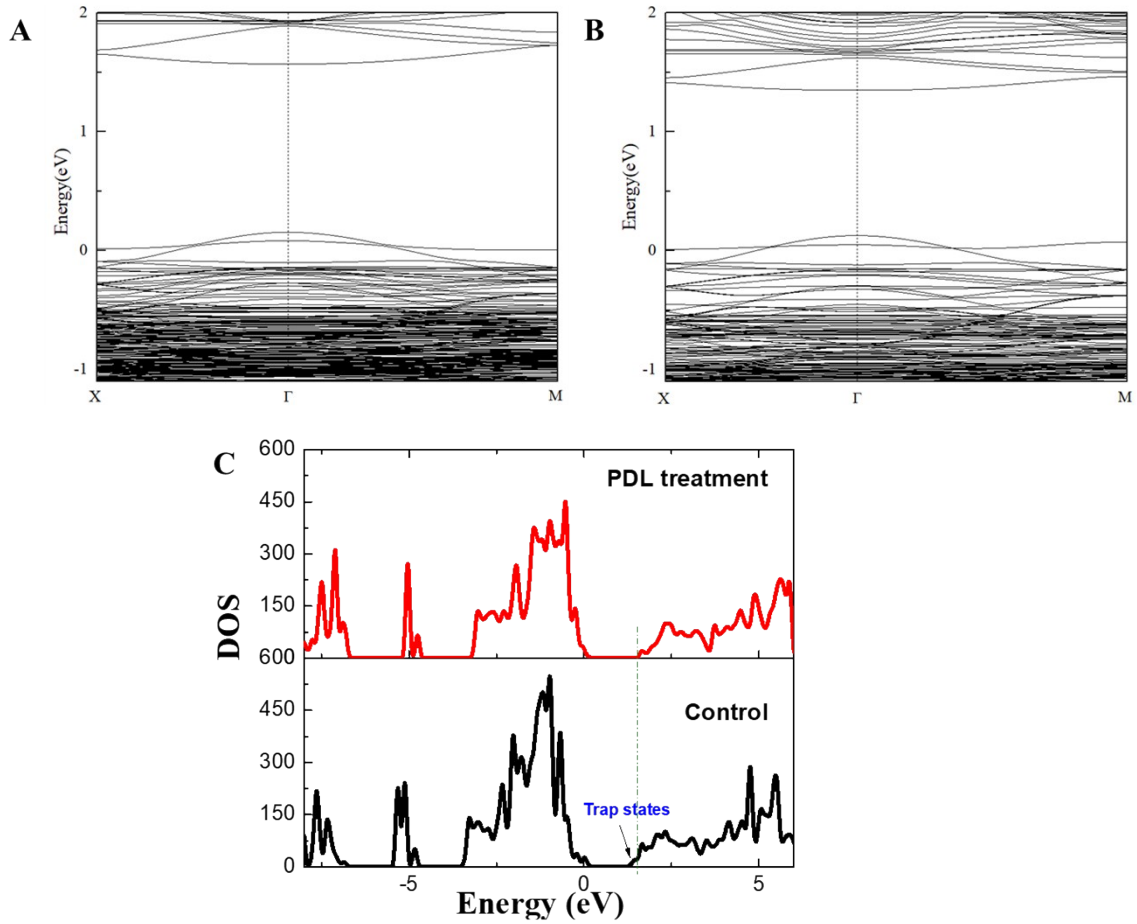

Fig. S13 Calculated band structure of PbI_2-terminated $MAPbI_3$ (a) without (b) with DETA passivation. (c) Projected density of states show the formation of trap states in the case of PbI_2-termination and an absence of trap states in the case of DETA passivated PbI_2-termination.

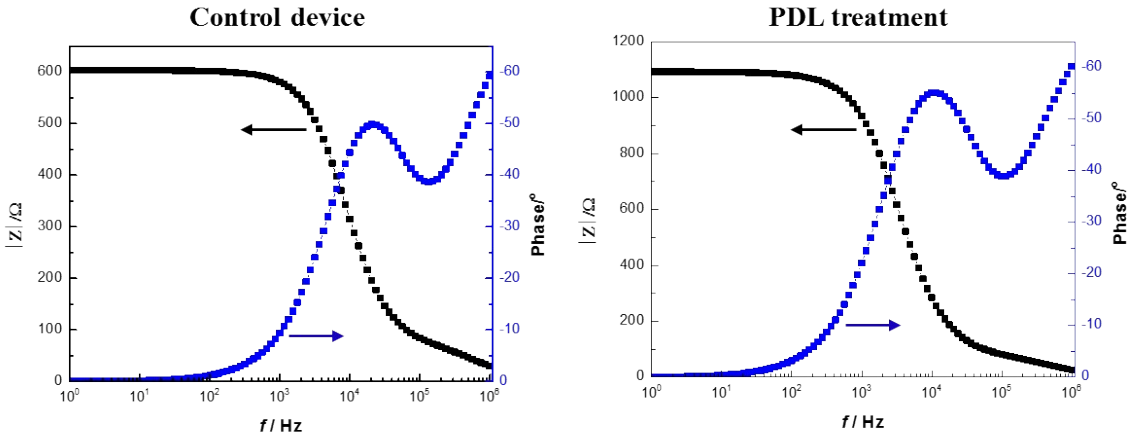

Fig. S14 Bode plot to the circuit shown in Fig. 4e.

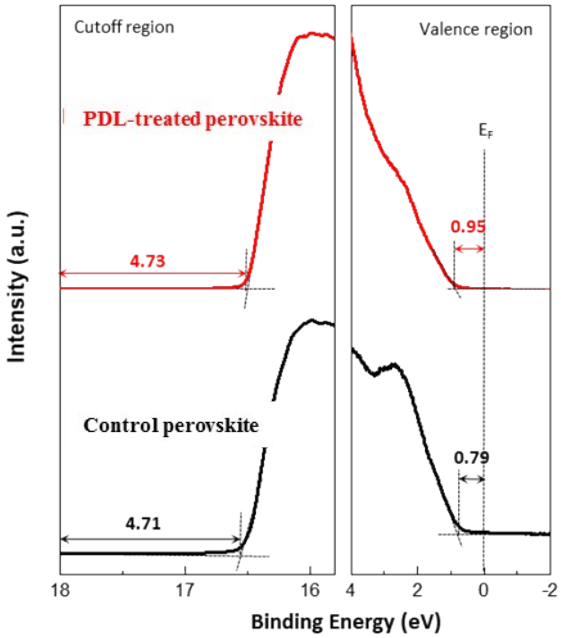

Fig. S15 Ultraviolet photoelectron spectra (UPS) of the control and PDL treated perovskite films.

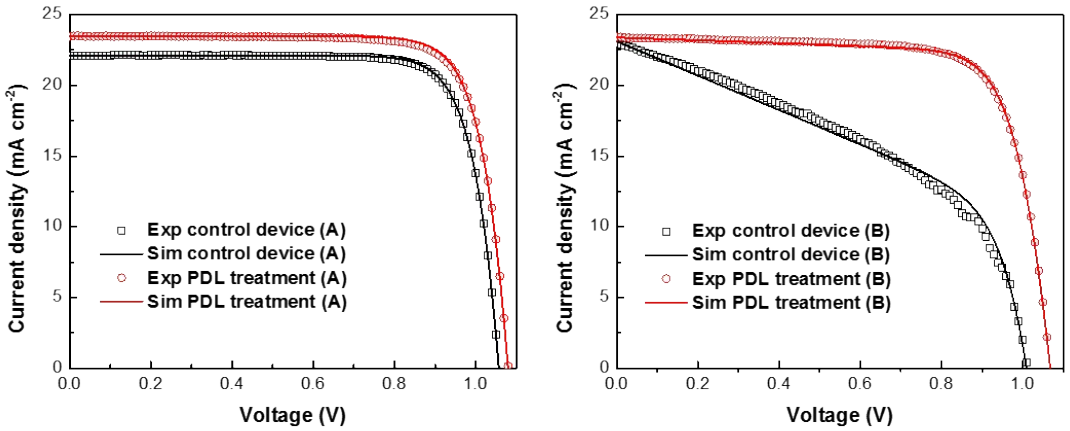

Fig. S16 Theoretically fitted and experimentally measured *J-V* characteristics for device A and device B.

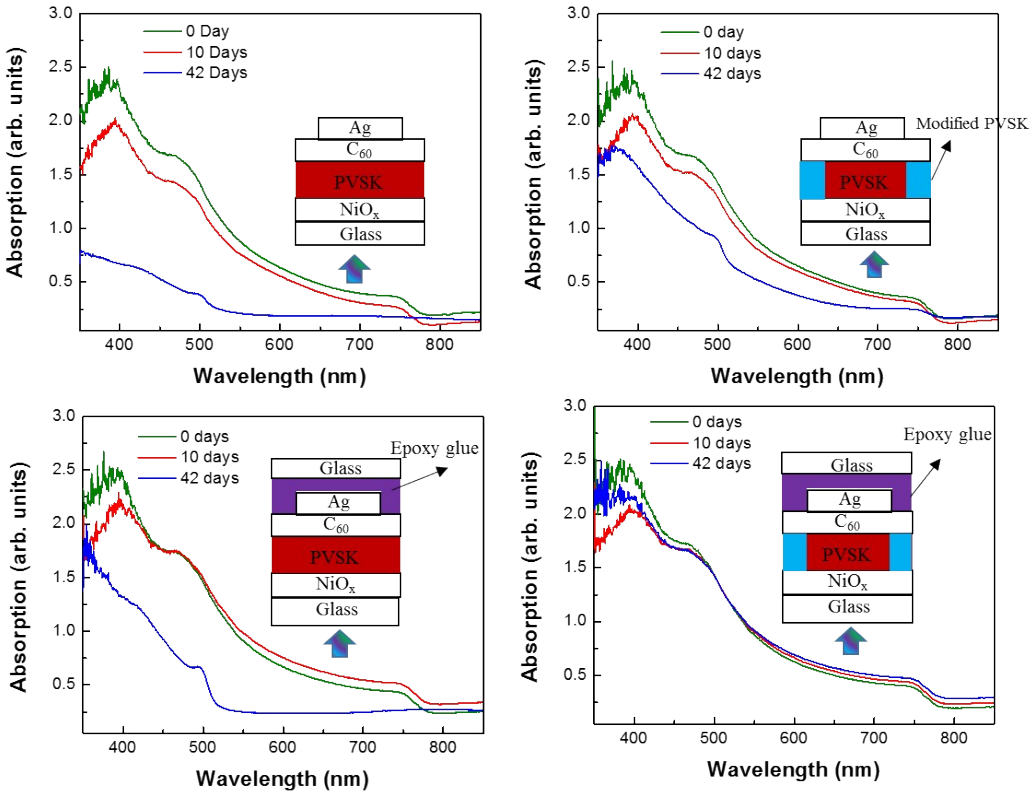

Fig. S17 Absorption spectra of (a) unencapsulated control device, (b) unencapsulated PDL treated device, (c) encapsulated control device, and (d) encapsulated PDL treated device with time. The devices were stored in ambient environment. The humidity and temperature are 50±5 % and 25±1 degC, respectively. The encapsulated devices were sealed by commercial epoxy glue.

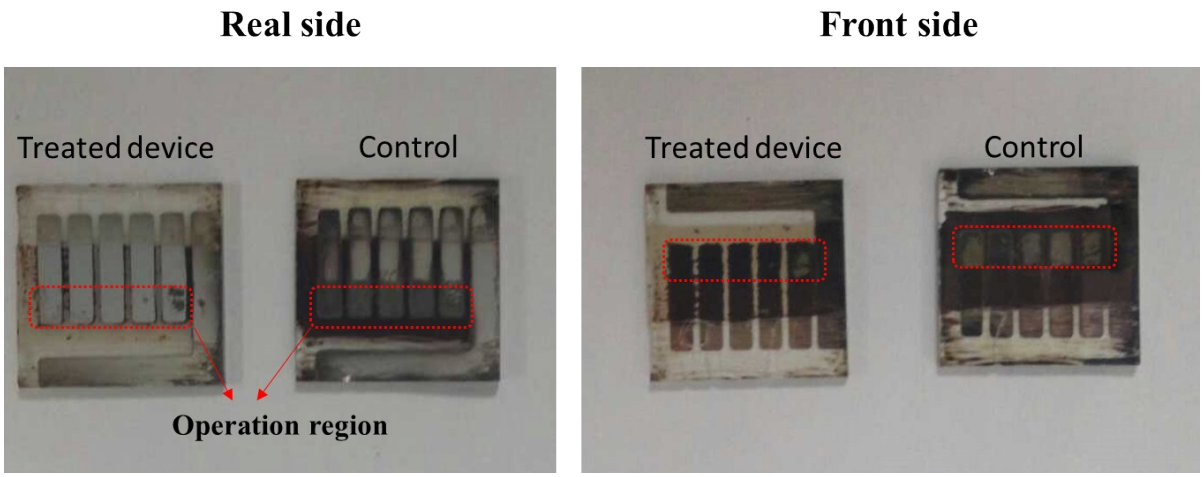

Fig. S18 Real photographs of PVSCs with and without PDL treatment after MPP tracking. The electrode is silver in the picture.

References:

[1] Lindblad et al., *J. Phys. Chem. Lett.* 2014, 5, 648.

[2] Haruyama et al., *J. Phys. Chem. Lett.* 2014, 5, 2903.

[3] Yin et al., *App. Phys. Lett.* 2014, 104, 063903.